32nd Annual International Conference of the IEEE EMBS
Buenos Aires, Argentina, August 31 - September 4, 2010

Automatic Liver Segmentation from CT Scans Based on a Statistical Shape Model

Xing Zhang, Jie Tian*, *Fellow, IEEE,* Kexin Deng, Yongfang Wu and Xiuli Li

Abstract— **In this paper, we present an algorithm for automatic liver segmentation from CT scans which is based on a statistical shape model. The proposed method is a hybrid method that combines three steps: 1) Localization of the average liver shape model in a test CT volume via 3D generalized Hough transform; 2) Subspace initialization of the statistical shape model; 3) Deformation of the shape model to adapt to liver contour through an optimal surface detection approach based on graph theory. The proposed method is evaluated on MICCAI 2007 liver segmentation challenge datasets. The experiment results demonstrate availability of the proposed method.**

I. INTRODUCTION

Computer-aided liver analysis can help reduce the risk of liver surgery and design treatment strategies. Accurate and robust segmentation of liver tissue from medical images is a prerequisite for liver analysis and diagnosis. Computed tomography (CT) volume is often used for liver segmentation and subsequent liver vessels segmentation. Due to highly varying shape of liver and weak edges among some neighboring organs, liver segmentation becomes a challenging task which attracts much research attention more recently. Remarkably, MICCAI 2007 Workshop on 3D liver segmentation provides a platform for testing and comparing different approaches for the topic [1]. In the competition, the statistical shape model (SSM) based method [2], [3] has the best performance among all approaches. As a matter of fact, SSM based approaches are proved available for liver segmentation by researchers.

The statistical shape model segmentation framework is first proposed by Cootes [4] *et al*. Techniques involved in the SSM include shape correspondence, shape representation and search algorithms. In the shape model construction step, establishing landmark points correspondence among all shapes of the training sets is generally the most challenging part. Spherical harmonics (SPHARM) [5] mapping for each training shape is an effective registration method for shape correspondence and the group-wise optimization strategy can produce better results than pair-wise method. Subsequently, a compact shape description via classical principal component analysis (PCA) can be applied for shape representation. In fact, SSM based approaches are sensitive to initialization of the model pose. Contrast to manual or the time-consuming evolutionary algorithm [6] proposed before, we present a 3D generalized Hough transform method to detect approximate location of the liver and then a subspace initialization based on intensity and gradient profile along the vertex normal is proposed. Finally, the shape model is deformed to adapt to the liver contour through an optimal surface detection based on graph theory.

This work is supported by NBRPC (2006CB705700), PCSIRT (IRT0645), CAS HTP, KIPCAS (KSCX2-YW-R-262, KGCX2-YW-129), NSFC (30873462, 60910006, 30970769, 30970771).

X. Zhang, J. Tian, K.-X. Deng, Y.-F. Wu, and X.-L. Li are with Medical Image Processing Group, Institute of Automation, Chinese Academy of Sciences, Beijing 100190, China. e-mail: tian@ieee.org

II. METHODS

A. Shape Model Construction

The liver shape model is built from several ground truth segmentation results. Shape model is always described as a point distribution model (PDM) which refers to the landmark points on an object surface. The PDM of the liver is represented by a triangulated mesh which is obtained via marching cubes algorithm. The key process of statistical shape model construction is establishing landmark points correspondence among all shapes of the training sets. A population-based method for points correspondence is minimizing description length (MDL) [7] of the generated model. For convenient manipulation, original triangulated mesh is mapped to a unit sphere by spherical harmonics (SPHARM)[5] parameterization. After alignment of all training triangulated meshes in a common coordinate system based on similarity transform (translation, rotation and scaling), the standard principal component analysis (PCA) is applied to represent variation modes of the training set. Each valid liver shape vector can be approximated by the average shape vector plus a subspace spanned by the first c ($c \le n$) eigenmodes:

$$\Phi \cong T^{-1}\left(\overline{\Phi} + \sum_{m=1}^{c} b_m p_m\right) \tag{1}$$

where $\overline{\Phi} = \sum_i \Phi_i / n$ is the average shape vector, p_m is the principal mode of variation obtained through PCA, b_m is the corresponding weight for each principal mode, T is a similarity transform computed from the given shape Φ to the average shape $\overline{\Phi}$. An instance of a SSM should have a limitation of $b_m \in \left[-3\sqrt{\lambda_m}, 3\sqrt{\lambda_m}\right]$ for not producing large deviation from the training sets, where λ_m is the corresponding eigenvalue for each eigenvector p_m. The variability of the liver shape model is displayed in Fig. 1.

B. Preprocessing

In order to reduce noise while preserving liver contour, a 3D nonlinear diffusion filter is applied to a test volume, the nonlinear diffusion equation is given as follows:

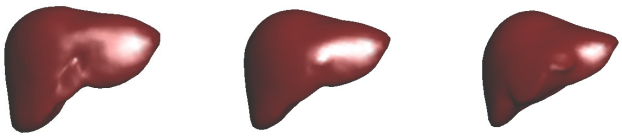

(a) (b) (c)

Fig. 1. Variability of a statistical model of the liver shape obtained from 40 training data sets. (a) The eigenmode with the largest variance $+\sqrt{\lambda_1}p_1$; (b) The averaged liver model $\bar{\Phi}$; (c) The eigenmode with the largest variance $-\sqrt{\lambda_1}p_1$.

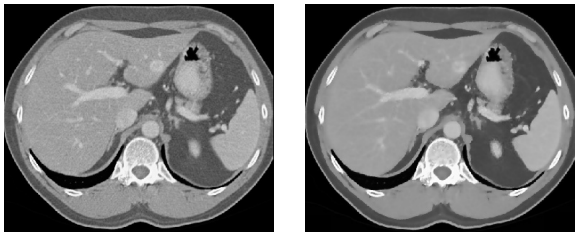

(a) (b)

Fig. 2. 3D nonlinear diffusion filtering. (a) Original transversal slice of liver before nonlinear diffusion; (b) Transversal images of liver after nonlinear diffusion.

$$\begin{cases} \frac{\partial u(x,y,z,t)}{\partial t} = div[g(|\nabla u|)\nabla u] \\ u(x,y,z,0) = u_0(x,y,z) \end{cases} \quad (2)$$

where the diffusivity function $g(s) = 1 - \exp\left(-3.315(\lambda/s)^8\right)$ if $s > 0$ and $g(s) = 1$ otherwise. The effect of the diffusion filter on a CT slice is illustrated in Fig 2.

C. Liver Localization by 3D Generalized Hough Transform

Liver localization is a prerequisite for accurate liver segmentation. This makes the average shape initialization in volume data a crucial step. Hough transform is an effective and robust method to detect any arbitrary shape in an image [8]. During GHT learning process, the triangulated mesh of the average shape model is employed as a template shape. As shown in Fig. 3, the liver centroid c is used as the reference point. For each vertex p on the surface, revolution angle α and azimuthal angle β of the vertex normal $\overrightarrow{n_p}$ is discretized as the entries of the 2D reference table (R-table). The R-table constructed by storing vector $\overrightarrow{r_p}$ for each vertex p is indexed by α and β, as shown in Fig. 3(b). When detecting liver shape in a test volume, the gradient angle α and β of an edge point is employed to retrieve corresponding entries of the R-table. An accumulator array for parameter space saves the votes of edge points to determine the most probable center of liver.

In order to reduce dimensionalities of the parameter space, we restrict the average shape model only transform under translation and isotropic scaling which neglects rotation. The transformation requires a 4D parameter space storage. The experiments show the assumption can effectively reduce computational cost while giving acceptable localization result. For an edge point $\overrightarrow{v_q}$ in a test volume, the corresponding $\overrightarrow{r_p}$ can be determined by gradient direction of the edge point. Then the possible location of reference point in the parameter space is calculated from $\overrightarrow{v_q} + s\overrightarrow{r_p}$, where s denotes the scaling factor.

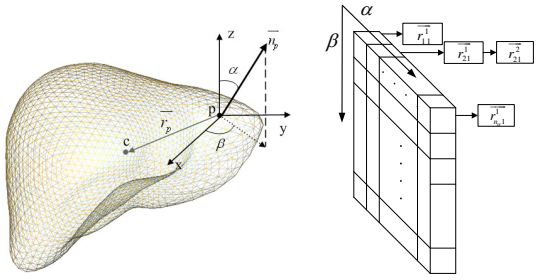

(a) (b)

Fig. 3. Parameters involved in the 3D GHT. (a) The revolution angle α and azimuthal angle β of the surface vertex normal is indexed as the entries of the R-table; (b) Illustration of a 2D R-table constructed by storing vector $\vec{r}$.

Before liver localization, the CT volume requires preprocessing. 1) Image downsampling: GHT is performed on the low resolution layer of the CT volume to capture global information while improving efficiency. The original CT image is downsampled to $3 \times 3 \times 3$ mm^3 using linear interpolation. Since the scale of the liver is more larger than the spacial sampling interval, shape of liver can be preserved well after downsampling process. 2) Image smoothing: In order to eliminate staircase edges resulted from downsampling, a mean filter is employed to smooth the downsampled CT volume. 3) Edge detection: The edges of the image is detected through Canny edge detector while pruning edges which definitely not belong to liver boundary. The liver has a CT value range of $\left[I_{low}, I_{high}\right]$, edges with corresponding CT value out of the range will be pruned for an accurate and fast GHT localization.

D. Subspace Initialization of the Statistical Shape Model

An instance of the SSM demands computing a similarity transformation T and shape parameters b_m in the Eq. (1). Each vertex on the mesh is adjusted by evaluating fitness on the basis of the image data. First the pose of the model is evaluated through a similarity transform T, then the displacement vector of the transformed model and the original averaged model is projected onto subspace in the Eq. (1) through multivariate linear regression method to give the optimal parameter b_m.

Designing an appropriate search strategy is very crucial. Suppose the CT value range of liver is $I_L = \left[I_{low}, I_{high}\right]$ and $g_{\max}$ denotes the maximum gradient magnitude of the liver boundary. For each vertex $\overrightarrow{v_i}$ on the mesh, candidate liver boundary point is searched along the vertex normal $\overrightarrow{n_i}$, N equidistant points are sampled along each vertex normal direction:

$$\overrightarrow{v_k} = \overrightarrow{v_i} + (k - \frac{N-1}{2}) \bullet d \bullet \overrightarrow{n_i} \qquad k = 0 \cdots N-1 \quad (3)$$

where d is the sampling distance. For an initial vertex v_k $(k = \frac{N-1}{2})$ on the mesh, if $I(v_k) \in I_L$ then count the number c of consecutive $i \le k$ with $I(v_i) \in I_L$, the vertex v_k is

considered inside liver when $c \geq c_{\text{thresh}}$, otherwise v_k outside liver. Based on these assumptions, two different strategies are used for searching candidate points:

1) v_k *is inside liver:* Search candidate points with $i \in \left[\frac{N-1}{2}, N-1\right]$, count number c of consecutive points $I(v_i) \in I_L$ and $|\nabla I(v_i)| \leq g_{\max}$, set $k = \frac{N-1}{2} + c$;
2) v_k *is outside liver:* Search candidate points with $i \in \left[0, \frac{N-1}{2}\right]$, count number c of consecutive points $I(v_i) \in I_L$ and $|\nabla I(v_k)| \leq g_{\max}$, set $k = c$.

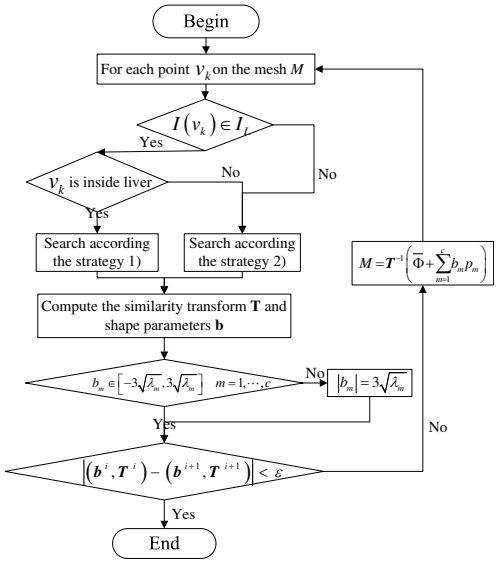

Fig. 4. The flowchart of the subspace initialization process.

The flowchart is illustrated as Fig. 4. For an initial mesh M generated from 3D GHT localization, search candidate point for each vertex and then compute the pose $\boldsymbol{T}$ and shape parameters $\boldsymbol{b}$ iteratively until convergence. The output of the step is $M = (T^*)^{-1}\left(\bar{\Phi} + Pb^*\right)$, where T^* and b^* are corresponding optimal solution of T and b.

E. Optimal Surface Detection Approach Based on Graph Theory

Since the segmentation result of the subspace initialization is just a linear combination of variation modes described in Eq. (1), which abundantly exploits prior of a typical liver shape, but lacks flexibility to adapt to a liver in an arbitrary test volume. Based on the previous segmentation result, we employ an optimal surface detection algorithm in the final refined segmentation process.

The optimal surface detection approach based on graph theory is first proposed by Li *et al* [9]. The method can globally optimize a cost function which incorporates sum of nodes cost and surface smoothness constraint by transforming it to a minimum s-t cut problem. Then a max-flow/min-cut algorithm [10] can be employed to solve the *s-t* cut problem in polynomial time. In this refined segmentation process, the segmentation result of the previous step is used as initialization.

The graph is constructed in a narrow-band around the segmented surface. Suppose a vertex $\vec{v_i}$ on the mesh and its normal $\vec{n_i}$, N equidistant points are sampled along each vertex normal direction for composing a column: $\vec{p_k} = \vec{v_i} + (k - \frac{N-1}{2}) \bullet d \bullet \vec{n_i}$ $(k = 0 \cdots N-1)$. As shown in Fig. 5 (b), there are two types of arcs in the graph, intra-column arcs and inter-column arcs. For each column in the graph, the intra-column arcs is defined as Eq. (4), the blue edges in Fig. 5 (b) denotes intra-column arcs.

$$E^a = \{\langle p_k, p_{k-1}\rangle \mid k = 1, \cdots, N-1\} \tag{4}$$

The inter-column arcs express the smoothness constraint. Consider two neighbouring columns P_m and P_n in the graph, the inter-column arcs is defined as Eq. (5), where the smoothness constraint Δ represents the maximum allowed difference between two neighbouring points on a surface. The green edges in Fig. 5 (b) denotes the inter-column arcs.

$$E^r = \{\left\langle p_k^m, p_{\max(0,k-\Delta)}^n \right\rangle \mid \forall P_m, P_n \text{ is adjacent}\} \tag{5}$$

Both the intra-column and inter-column arcs are regarded as n-links in graph and assign infinity. In the weighted directed graph, each node has a weight $w(v_k)$. Nodes with $w(v_k) \geq 0$ are connected to the sink node by a directed edge of weight $w(v_k)$, while nodes with $w(v_k) < 0$ are connected to the source node by a directed edge of weight $-w(v_k)$. The weight w_k^m of k*th* point in the m*th* column is defined as Eq. (6). The cost function c used in the Eq. (6) is negative gradient magnitude $c(v_k) = -|\nabla I(v_k)|$ if $I(v_k) \in I_L$ and $c(v_k) = 1$ otherwise. The negative gradient magnitude $c(v_k)$ is computed in image domain and then the node cost is derived by linear interpolation according to coordinate of the node.

$$w_k^m = \begin{cases} c_k^m & k = 0, \\ c_k^m - c_{k-1}^m & otherwise. \end{cases} \tag{6}$$

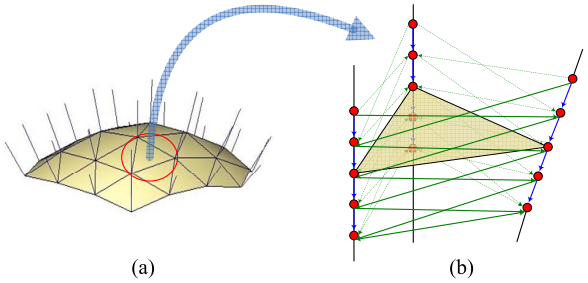

Fig. 5. Graph Construction. (a) A triangulated surface mesh with vertex normals; (b) Graph is constructed with intra-column and inter-column arcs. The blue edges denotes intra-column arcs while green edges denotes inter-column arcs. Smoothness constraint in this graph is $\Delta = 1$.

III. EXPERIMENTS AND RESULTS

The proposed method is tested on the training datasets of MICCAI 2007 liver segmentation challenge. There are 20 CT volumes of abdomen with contrast agent in the training datasets. All datasets have an in-plane resolution of 512×512 pixels and inter-slice spacing from 0.7 mm to 5.0 mm. Other 40 CT volume with normal liver anatomy obtained clinically

TABLE I

PARAMETERS SELECTION

Step	Parameters
1. Nonlinear diffusion filtering	$\lambda = 30$, $\Delta t = 0.15$, t = 1.5
2. 3D GHT	$\Delta\alpha = \frac{\pi}{20}$, $\Delta\beta = \frac{\pi}{20}$, scaling factor $s \in [0.9, 1.0, 1.1]$, $\left[I_{low}, I_{high}\right] = [50, 200]$
3. Subspace initialization	sampling distance d=1 mm, sampling points N = 41, $c_{\text{thresh}} = 10$, $\varepsilon = 2$, $g_{\max} = 200$, all 40 variation modes are used
4. Optimal surface detection	sampling distance d=1 mm, sampling points N = 31, smoothness constraint $\Delta = 2$

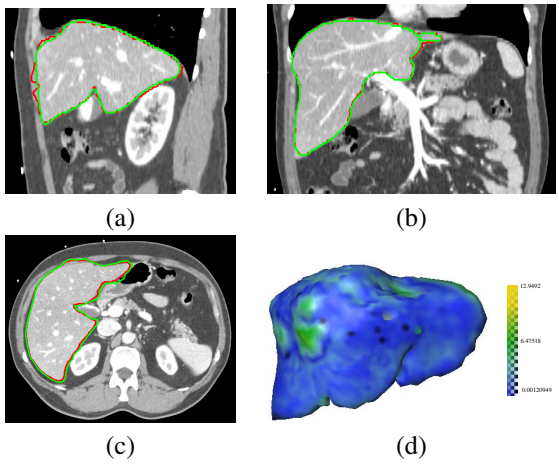

Fig. 6. The contour of the expert manual reference segmentation is in green, the contour of the segmentation of the method described in this paper is in red. (a), (b) and (c) are sagittal, coronal and transversal slice from a test CT volume respectively; (d) Surface distance map from the segmentation result to the reference result.

are used for shape model construction with 2562 equally distributed vertices on each model.

A. Segmentation Workflow and Parameters Selection

The segmentation workflow consists of following steps: 1. Nonlinear diffusion filtering; 2. Average model localization through 3D GHT; 3. Model subspace initialization; 4. Refined segmentation based on optimal surface detection. The parameters for each step are listed in Table I.

B. Results

The resulting surface meshes are converted to volume with the same dimension and spacing as the corresponding CT volume datasets. Fig. 6 shows the final segmentation results with comparison to expert manual reference segmentation. The segmentation results are compared to the ground truth results according to volumetric overlap error (Overlap Error), symmetric average surface distance D_{Avg} and symmetric RMS surface distance D_{RMS}. The three average segmentation results metrics of 20 training datasets achieved by the proposed method are summarized in Table II in comparison with previous works from literature.

TABLE II

RESULTS OF THE COMPARISON METRICS WITH PREVIOUS WORK

	Overlap Error[%]	$D_{\text{Avg}}[mm]$	D_{RMS} $[mm]$
Kainmueller[2]	6.09 ± 2.13	0.63 ± 0.11	1.22 ± 0.22
Heimann[6]	5.1 ± 1.4	1.6 ± 0.5	3.3 ± 1.2
Lamecker[11]	7.0 ± 1.8	2.3 ± 0.3	3.1 ± 0.5
Our approach	5.25 ± 0.91	0.93 ± 0.25	2.23 ± 1.04

IV. FUTURE WORKS

The paper presents a hybrid method based on statistical shape model to perform automatic liver segmentation from CT scans. The experiments demonstrate availability of the proposed method. There are two important future works along our study: more training datasets will be involved in shape model construction and improve efficiency of some processing steps. Though 3D GHT provides acceptable liver localization of the average shape model just under translation and isotropic scaling, the major weakness of GHT is that the scale and rotation of the object is handled in a brute-force manner which requires a 6D parameter space and high computational cost. An orientation and scale-invariant GHT method may solve the problem. The subspace initialization step proceeds iteratively and the candidate points searching process takes most of the time but it can be parallelized for acceleration.

REFERENCES

[1] T. Heimann, B. van Ginneken, M. Styner, Y. Arzhaeva, V. Aurich and *et al.*, "Comparison and Evaluation of Methods for Liver Segmentation From CT Datasets", *IEEE Trans. Med. Imaging.*, vol. 28, no. 8, 2009, pp. 1251-1265.

[2] D. Kainmueller, T. Lange and H. Lamecker, "Shape Constrained Automatic Segmentation of the Liver based on a Heuristic Intensity Model", *in MICCAI Workshop. 3D Segmentation in the Clinic: A Grand Challenge*, 2007, pp. 109-116.

[3] T. Heimann and H.-P. Meinzer, "Statistical shape models for 3D medical image segmentation: A review", *Med. Image Anal.*, vol. 13, 2009, pp. 543-563.

[4] T.-F. Cootes, C.-J. Taylor, D.-H. Cooper and J. Graham, "Active Shape Models-Their Training and Application", *Comput. Vis. Image Underst.*, vol. 61, no. 1, 1995, pp. 38-59.

[5] A. Kelemen, G. Szekely and G. Gerig, "Elastic Model-based Segmentation of 3-D Neuroradiological Data Sets", *IEEE Trans. Med. Imaging.*, vol. 18, no. 10, 1999, pp. 828-839.

[6] T. Heimann, S. Munzing, H.-P. Meinzer, and I. Wolf, "A Shape-Guided Deformable Model with Evolutionary Algorithm Initialization for 3D Soft Tissue Segmentation", *in Proceedings of the International Conference on Information Processing in Medical Imaging 2007 (IPMI07)*, Kerkrade, vol. 4584, 2007, pp. 1-12.

[7] R.-H. Davies, C.-J. Twining, T.-F. Cootes, J.-C. Waterton and C.-J. Taylor, "A Minimum Description Length Approach to Statistical Shape Modelling", *IEEE Trans. Med. Imaging.*, vol. 21, no. 5, 2002, pp. 525-537.

[8] K. Khoshelham, "Extending Generalized Hough Transform to Detect 3D Objects in Laser Range Data", *in ISPRS Workshop on Laser Scanning*, Espoo, Finland, 2007, pp. 206-210.

[9] K. Li, X. Wu, D.-Z. Chen, and M. Sonka, "Optimal Surface Segmentation in Volumetric ImagesłA Graph-Theoretic Approach", *IEEE Trans. Pattern Anal. Mach. Intell.*, vol. 28, no. 1, 2006, pp. 119-134.

[10] Y. Boykov and V. Kolmogorov, "An Experimental Comparison of Min-Cut/Max-Flow Algorithms for Energy Minimization in Vision", *IEEE Trans. Pattern Anal. Mach. Intell.*, vol. 26, no. 9, 2004, pp. 1124-1137.

[11] H. Lamecker, T. Lange and M. Seebaee, "Segmentation of the Liver using a 3D Statistical Shape Model", *ZIB Tech. Report*, Zuse Institue, Berlin, 2004.